Carbohydrate Polymers 81 (2010) 196–202

Contents lists available at ScienceDirect

Carbohydrate Polymers

journal homepage: www.elsevier.com/locate/carbpol

Development of semi-interpenetrating carbohydrate polymeric hydrogels embedded silver nanoparticles and its facile studies on *E. coli*

V. Ramesh Babu[a], Changdae Kim[b], Sangsu Kim[c], Chuljin Ahn[a], Yong-Ill Lee[a,*]

[a] Department of Chemistry, Changwon National University, 9 Sarim Dong, Changwon 641-773, Republic of Korea
[b] Department of Physics, Mokpo National University, Muan 534-729, Republic of Korea
[c] Department of Physics, Changwon National University, Changwon 641-773, Republic of Korea

ARTICLE INFO

Article history:
Received 3 November 2009
Accepted 9 February 2010
Available online 10 March 2010

Keywords:
Carbohydrate polymers
Chitosan
Silver nanoparticles
Antibacterial study
Semi-interpenetrating polymer network

ABSTRACT

Semi-interpenetrating carbohydrate polymer network [semi-IPN] hydrogels are composed with combination of carbohydrate polymers, chitosan and sodium alginate with 2-hydroxyethyl methacrylate. The semi-IPN carbohydrate hydrogels were successfully synthesized by using free radical polymerization technique. Silver nanopaticles were formed by reduction of silver nitrate in semi-IPN carbohydrate hydrogels with sodium borohydrate under room temperature. The formation of silver nanoparticles in hydrogels were well characterized by using UV–visible spectroscopy, thermo gravimetrical analysis, X-ray diffractrometry studies, scanning electron microscopy and transmission electron microscopy studies. Thermal and X-ray driffraction analysis confirmed the formation of silver nanoparticles in semi-IPN hydrogel. SEM images indicated clearly the formation of group of silver nanoparticles with size range of 10–20 nm. The sizes of silver nanoparticles were also supported by transmission electron microscopy results. The silver nanoparticles in semi-IPN hydrogel showed very good antibacterial activity on *Escherichia coli*, thus it reveals that the silver nanoparticles are acting as excellent antibiotics.

1. Introduction

Polysaccharides, a class of naturally available carbohydrate polymers, have been used extensively in food industry as gelling agents and for encapsulation of living cells (Cai, Shi, Sherman, & Sun, 1989; Hertzberg, Moen, Vogelsang, & Oestgaard, 1995; Lim & Moss, 1981; Ramesh Babu, Sairam, Hosamani, & Aminabahvi, 2007; Ramesh Babu, Hosamani, & Aminabahvi, 2008). Sodium alginate (NaAlg), a natural polysaccharide, composed of D-mannuronic acid and D-guluronic acid, is derived from the brown seaweeds. NaAlg is a biodegradable polymer used extensively in drug delivery applications (Aminabhavi, Kulkarni, Soppimath, Dave, & Mehta, 1999; Downs, Robertson, Riss, & Plunkett, 1992; Babu et al., 2006). Chitosan (CS) which can be obtained from the deacetylation of chitin is one of the most facile polymers, whose structure can be modified chemically (Park, You, Park, Haam, & Kim, 2001; Binder & Heinrich, 2000). It is more widely used in biomedical applications than chitin itself because it degrades in an aqueous environment because of the presence of hydroxyl and aminogroups which can be readily modified (Kang, Choi, & Kweon, 1999; Peniche et al., 1999). The key characteristics of CS in such applications are its biocompatibility, nonantigenicity, nontoxicity (its degradation products are well-known natural metabolites), ability to improve wound healing and blood clotting and ability to absorb liquids and thus form protective films and coatings, etc. (Lee & Chen, 2001). Poly(hydroxyethyl methacrylate) (PHEMA) has good biocompatibility and mechanical strength required for biomedical applications. PHEMA is a hydrogel that swells but is insoluble in water and hence, it possesses the ability to retain water within its structure (Ng, Yuan, & Zhao, 1998; Sastre, Blanco, Gomez, Socorro, & Teijon, 1999).

Embedding colloidal nanoparticles into polymer matrices is an effective method for enhancing the functions of colloidal particles (Whitcombe & Vulfson, 2001). Such an inorganic/polymeric hybrid network combines the advantages of both polymer and nanoparticles. Recently, strategies have been developed to obtain functional metal or metal iron–polymer hybrid systems that exhibit tailored electronic properties (Chegel et al., 2002). The application of nanoscale materials and structures, usually ranging from 1 to 100 nanometers (nm), is an emerging area of nanoscience and nanotechnology. Nanomaterials may provide solutions to technological and environmental challenges in the areas of solar energy conversion, catalysis, medicine and water treatment (Hutchison, 2008; Dahl, Bettye, Maddux, & Hutchison, 2007). This increasing demand must be accompanied by "green" synthesis methods. In the global efforts to reduce generated hazardous waste, "green" chemistry and chemical processes are progressively integrating with modern developments in science and industry. Implementation of these sustainable processes should adopt the 12 fundamental prin-

* Corresponding author. Tel.: +82 55 213 3436; fax: +82 55 213 3439.
E-mail address: yilee@changwon.ac.kr (Y.-I. Lee).

0144-8617/$ – see front matter © 2010 Elsevier Ltd. All rights reserved.
doi:10.1016/j.carbpol.2010.02.050

ciples of green chemistry (Anstas & Warner, 1998; Cross & Kalra, 2002; DeSimone, 2002; Poliakoff & Anastas, 2001; Raveendran, Fu, & Wallen, 2003). These principles are geared to guide in minimizing the use of unsafe products and maximizing the efficiency of chemical processes. Hence, any synthetic route or chemical process should address these principles by using environmentally benign solvents and nontoxic chemicals.

Generally, metal nanoparticles can be prepared and stabilized by physical and chemical methods; the chemical approach including chemical reduction, electrochemical techniques, and photochemical reduction is most widely used (Chen, Cai, Zhang, Wang, & Zhang, 2001). Studies have shown that the size, morphology, stability and properties (chemical and physical) of the metal nanoparticles are strongly influenced by the experimental conditions, the kinetics of interaction of metal ions with reducing agents, and adsorption processes of stabilizing agent with metal nanoparticles (Knoll & Keilmann, 1999; Shiladitya et al., 2005). Therefore, the design of a synthesis method in which the size, morphology, stability and properties can be controlled has become a major field of interest (Wiley, Sun, & Xia, 2007).

Chemical reduction is the most frequently applied method for the preparation of silver nanoparticles (Ag NPs) as stable, colloidal dispersions in water or organic solvents (Wiley, Sun, Mayers, & Xia, 2005). Commonly used reductants are borohydride, citrate, ascorbate, and elemental hydrogen (Chou & Ren, 2000; Nickel, Castell, Poppl, & Schneider, 2000; Shirtcliffe, Nickel, & Schneider, 1999; Frattini, Pellegri, Nicastro & DeSanctis, 2005). The reduction of silver ions (Ag^+) in aqueous solution generally yields colloidal silver with particle diameters of several nanometers (Wiley et al., 2005). Initially, the reduction of various complexes with Ag^+ ions leads to the formation of silver atoms (Ag), which is followed by agglomeration into oligomeric clusters (Kapoor, Lawless, Kennepohl, Meisel, & Serpone, 1994). These clusters eventually lead to the formation of colloidal Ag particles. When the colloidal particles are much smaller than the wavelength of visible light, the solutions have a yellow color with an intense band in the 380–400 nm range and other less intense or smaller bands at longer wavelength in the absorption spectrum. This band is attributed to collective excitation of the electron gas in the particles, with a periodic change in electron density at the surface (surface plasmon absorption) (Henglein, 1989; Tao, Sinsermsuksakul, & Yang, 2006).

2. Experiments and materials

2.1. Materials

Chitosan, 2-hydroxyethyl metahcrylate (HEMA), *N*,*N*′-methylenebisacrylamide (MBA), ammonium persulfate (APS) were purchased from Aldrich, USA. *N*′,*N*′,*N*′,*N*′-Tetramethylethylenediamine (TEMED) was purchased from Alfa Aesar A Johnson Matthey Company. Sodium alginate was purchased from s.d. Fine chemicals, Mumbai, India. Sodium borohydride ($NaBH_4$) was purchased from Acros organics. Silver nitrate ($AgNO_3$) was purchased from Sigma–Aldrich, USA. To synthesize semi-IPN hydrogels, chitosan (1 g/10 ml), sodium alginate (1 g/10 ml), MBA (1 g/100 ml), APS (5 g/100 ml), TMEDA (1 g/100 ml), silver nitrate ($AgNO_3$) (8.493 g/500 ml), and sodium borohydrate (1.8915 g/500 ml) solutions were made in double-distilled water.

2.2. Preparation of semi-IPN hydrogels

Various amounts of chitosan and sodium alginate were weighed and dissolved under constant magnetic stirring in 2% acetic acid solution, distilled water, respectively overnight. To this solution, 1 ml of 2-hydroxyethyl metahcrylate, different amounts of crosslinker (MBA) (i.e., 10, 20 and 30 mg), initiating mixture (1 ml of APS/1 ml of TEMED) solutions were added and stirred well for 2 h to polymerize the monomer in 50 ml beaker at room temperature. The polymerization was carried out at room temperature over 24 h to form hydrogels. The synthesized hydrogels are washed with distilled water thrice to remove excess of adhered monomers. The washed gels are dried under vacuum for 24 h. All the formulations are given in Table 1.

Table 1
Formulation composition of semi-IPM hydrogel, nanocomposite.

Code	HEMA	NaAlg (mg)	MBA (mg)
NAHEMA-1	1 ml	200	10
NAHEMA-2	1 ml	600	10
NAHEMA-3	1 ml	800	10
NAHEMA-4	1 ml	200	20
NAHEMA-5	1 ml	200	30
Code	**HEMA**	**Chitosan (mg)**	**MBA (mg)**
CSHEMA-1	1 ml	200	10
CSHEMA-2	1 ml	600	10
CSHEMA-3	1 ml	800	10
CSHEMA-4	1 ml	200	20
CSHEMA-5	1 ml	200	30

2.3. Preparation of semi-IPN hydrogel–silver nanocomposites

To prepare semi-IPN hydrogel–silver nanocomposites, accurately weighed dry semi-IPN carbohydrate hydrogels were equilibrated in double-distilled water for 3 days and these semi-IPN carbohydrate hydrogels were transferred into a another beaker containing 50 ml of 5 mM $AgNO_3$ solution and allowed to equilibrate for 1 day. In this case, most of the silver ions are exchanged from solution into hydrogel networks by through $-COONa^+$, $-CONH_2$, –OH groups of hydrogel chains and rest of metal ions were occupied in free-network spaces of hydrogels. These silver salt loaded semi-IPN carbohydrate hydrogels were finally transferred into a beaker containing 50 ml of 10 mM $NaBH_4$ aqueous solution and allowed for 2 h to reduce the silver ions into silver nanoparticles. The obtained silver nanoparticles in the semi-IPN carbohydrate hydrogels are often termed in the forthcoming sections as semi-IPN hydrogel–silver nanocomposites.

2.4. Swelling studies

Fully dried semi-IPN carbohydrate hydrogels, silver nanocomposites were accurately weighed and equilibrated in distilled water at 37 °C for 3 days. The equilibrium swelling capacity or swelling ratio (Q) of the hydrogel was calculated employing following Eq. (1):

$$Q = \frac{W_e}{W_d} \quad (1)$$

where, W_e is the weight of swollen hydrogel and W_d is the dry weight of the semi-IPN hydrogel.

2.5. Antibacterial activity studies

Antibacterial studies of placebo semi-IPN hydrogel and its silver nanocomposite hydrogel were tested by paper disc method using *Escherichia coli*. 5 ml of nutrient agar (NA) medium (pH 6.8) was poured into the sterilized plates and allowed to solidify. The plates were inoculated with spore suspensions of *E. coli* (ATCC 10798) and paper discs (8 mm diameter) were dug inside the culture plates by using a sterilized cork borer. The test hydrogel solutions were prepared in distilled water. 20 μl of test solution was added to the discs and the plates were incubated at

37 °C for 24 h. The inhibition zone appeared around the disc was measured and recorded as the antibacterial effect of silver nanoparticles.

2.6. Characterization

UV–visible spectra of semi-IPN hydrogel–silver nanocomposites (10 mg in 1 ml of distilled water) were accomplished using Agilent 8453 UV spectrophotometer. X-ray diffraction measurements were carried out using X'pert MPD 3040 to know the crystallanity of the hydrogel. The thermal properties of semi-IPN carbohydrate hydrogels were evaluated by using TA 5000/SDT 2960 DSC Q10 thermal system (Zurich, Switzerland) at a heating rate of 10 °C/min under nitrogen atmosphere (flow rate 10 ml/min). Morphological variations of dry hydrogel, hydrogel–silver nanocomposites were studied by using a MIRA LMH, H.S. scanning electron microscope (SEM), operating at an acceleration voltage of 15 kV, coated with a thin layer of palladium gold alloy. Transmission electron microscopy (TEM) images of hydrogel–silver nanocomposites were recorded using a JEM 2100F transmission electron microscope. Particle size of silver nanoparticles was performed out by using zetasizer E, Malvern instruments.

3. Results and discussion

In present invention, authors have successfully produced silver nanoparticles in semi-IPN hydrogel system. At this point, we have designed, semi-IPN carbohydrate hydrogels employing sodium alginate, chitosan carbohydrate polymers which are renewed materials to enhance the reduction potential/anchoring ability and stabilization of the formed nanoparticles.

In any conventional hydrogel networks processes, the available functional groups and crosslink density decide the stability of nanoparticles. Therefore, in this invention, we have developed smaller size and narrow distributed silver nanoparticles in semi-IPN hydrogel networks prepared from of 2-hydroxyethyl methacrylate with NaAlg/CS carbohydrate polymeric chains. These hydrogel networks hold large amounts of metal ions in their network by anchoring the ions through carboxylic, amide and hydroxyl groups of carbohydrate polymers. The carbohydrate polymers in hydrogel networks arrest the agglomeration of silver nanoparticles.

3.1. Swelling studies

Fig. 1 shows the influence of ratios of carbohydrate polymer and crosslinking agent on the swelling characteristics of the hydrogels and silver nanocomposites. Considerable variation in the swelling capacity of semi-IPN carbohydrate hydrogels was noted when the hydrogels were modified or loaded with Ag salt and Ag nanoparticles. The order of swelling capacity values was found as silver nanocomposite hydrogel > semi-IPN hydrogel hydrogels. The swelling behavior of gels has varied with varying amount of crosslinking agent. As the amount of crosslinking agent increases, the swelling has been decreased due to high crosslink density and tightening of the polymeric chains which will become rigid structure of the polymer. However, the swelling ratio (g/g) of the silver nanocomposite hydrogels containing 10, 20, and 30 mg of crosslinking agent are 5.5, 4.3 and 3.4, respectively for CSHEMA

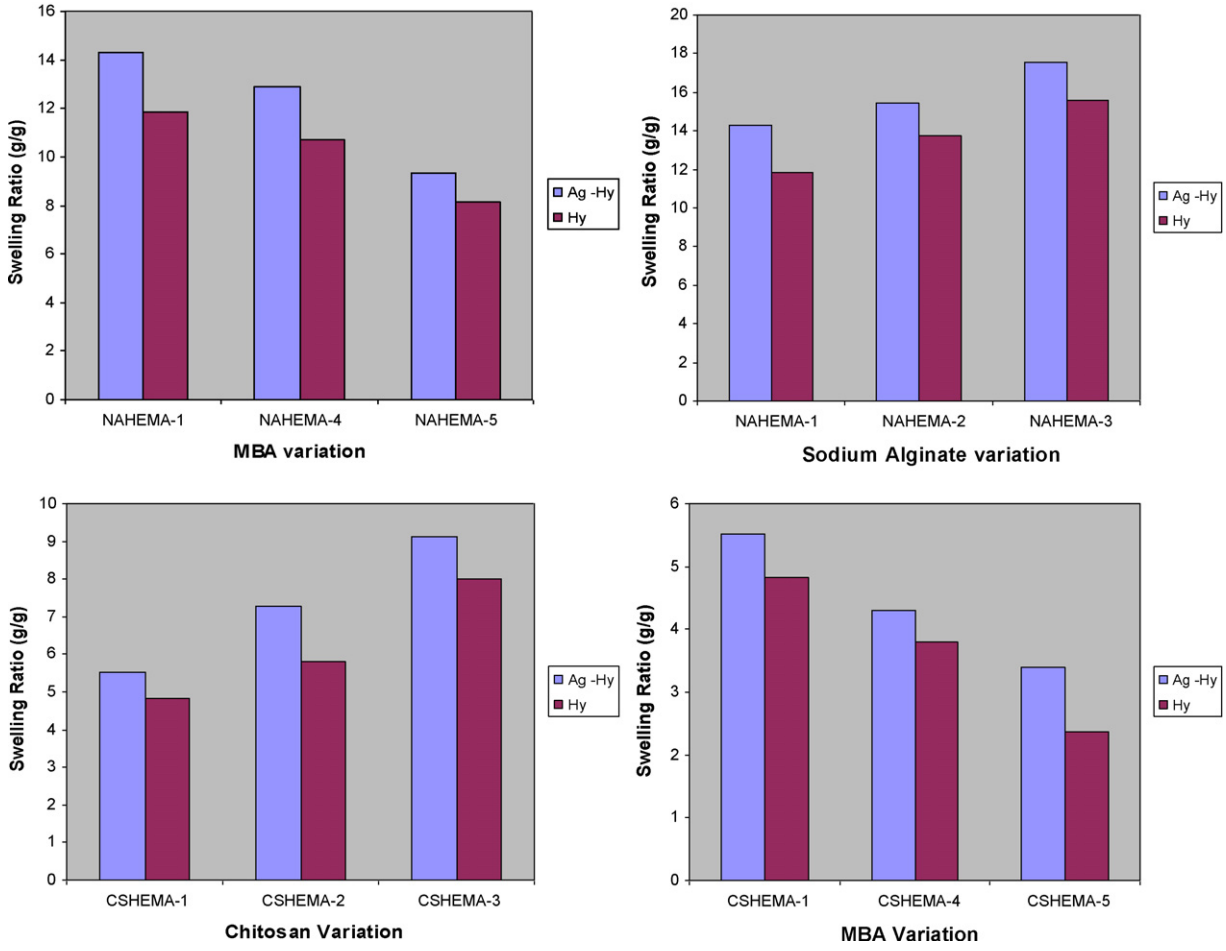

Fig. 1. Swelling behavior of pristine semi-IPN carbohydrate hydrogel and silver nanocomposite hydrogels of various formulations.

hydrogels and 14.4, 12.8 and 9.3, respectively for NAHEMA hydrogels. In case of sodium alginate and chitosan ratio in the hydrogel formation, swelling ratio increases with increasing the amount of sodium alginate and chitosan. This is fact due to the increase in hydrophilicity of the semi-IPN hydrogel matrix, which enhances the swelling ratio.

3.2. UV–visible spectroscopy

The formation of silver nanoparticles through semi-IPN hydrogel networks can be expected in our current strategy because the silver salts loaded in semi-IPN carbohydrate hydrogels are readily reduced by $NaBH_4$, which immediately turn into brown color. This indication of color change represents that the particles were entrapped inside the networks through strong localization and stabilization established by the carbohydrate polymers. The existence of silver nanoparticles in the gel networks were characterized by UV–visible spectroscopy analysis. Fig. 2 illustrates the absorption peaks of semi-IPN hydrogel–silver nanocomposites in 380–500 nm range that are assigned to silver nanoparticles which arose from the surface plasmon resonance (SPR) (Acharya et al., 2009). To investigate the reduction and stabilization efficiency of silver nanoparticles by hydrogel networks, authors studied UV–visible spectral analysis for silver nanocomposites. A significant improvement in the absorption peaks at 425 nm was observed hydrogels having sodium alginate and chitosan ratio. These polymeric variations with increase of NaAlg and CS content from 200 to 800 mg facilitate in holding large number of silver ion which were further reduced to silver nanoparticles.

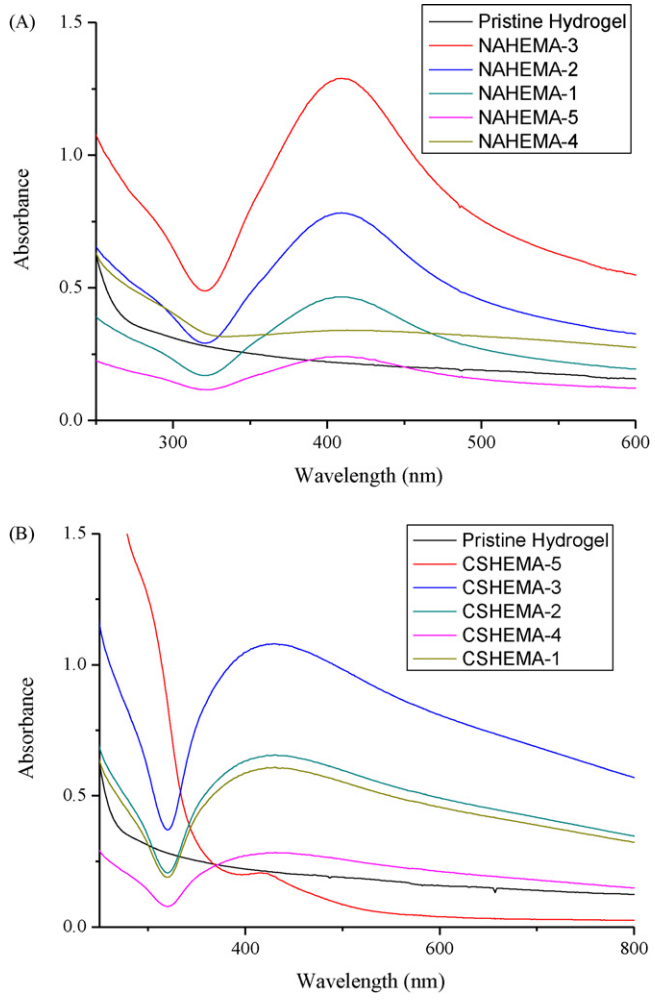

Fig. 2. UV–visible spectra of pristine semi-IPN carbohydrate hydrogel and silver nanocomposite hydrogels of various formulations.

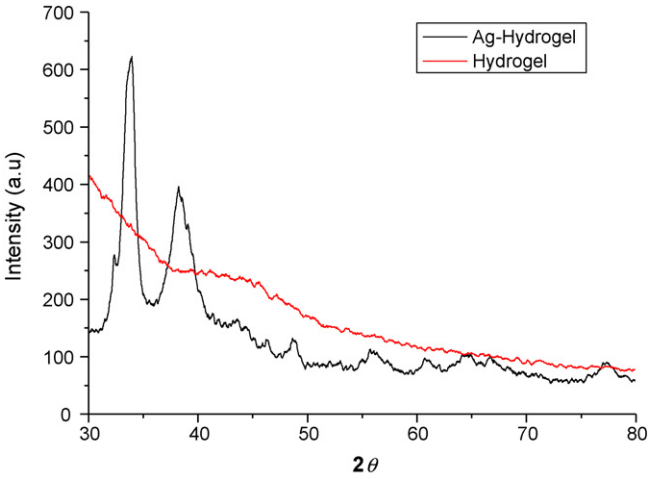

Fig. 3. XRD patterns of pristine semi-IPN carbohydrate hydrogel and silver nanocomposite hydrogels (NAHEMA-3).

3.3. X-ray diffraction

The crystallographic nature of the silver nanoparticles in hydrogels was investigated by X-ray diffraction. The X-ray diffraction patterns of pristine semi-IPN hydrogel and semi-IPN hydrogel–silver nanocomposite were demonstrated in Fig. 3. The diffractogram of semi-IPN hydrogel–silver nanocomposites are assigned to diffractions at 2θ values of about 34° and 38° plane of face centered cubic (fcc) structure of silver nanoparticles. The intense peaks represent to highly crystalline silver nanostructures formed in semi-IPN nanocomposites hydrogel. In pristine hydrogel there is no peaks are observed, this is due to the amorphous nature of carbohydrate semi-IPN hydrogel.

3.4. Thermal gravimetrical analysis

The silver nanocomposite hydrogels are characterized by thermo gravimetrical analysis to determine percentage of weight loss of hydrogel as well as silver nanoparticles in the hydrogel matrix. Fig. 4 shows the percentage decomposition of hydrogel

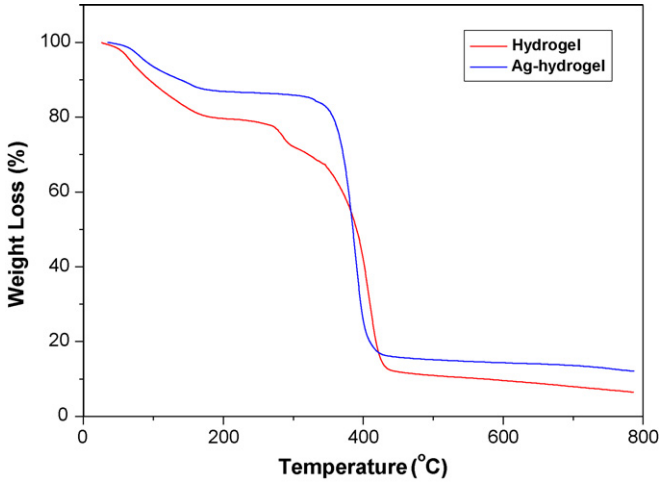

Fig. 4. Thermograms of pristine semi-IPN carbohydrate hydrogel and silver nanocomposite hydrogels (NAHEMA-3).

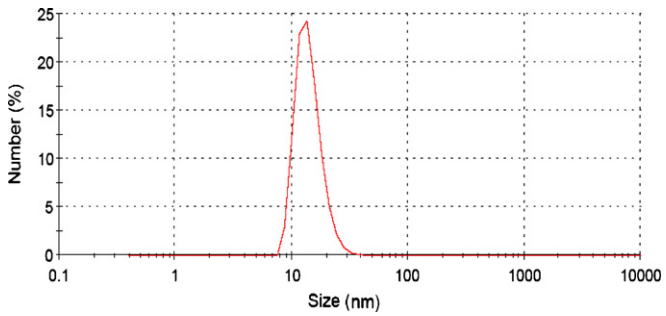

Fig. 5. Particle size analysis of silver nanoparticles extracted from (NAHEMA-3) silver nanocomposite hydrogels.

and silver nanocomposite hydrogel. The hydrogel has followed two decomposition steps and 95% degradation of the hydrogel chains occurred below 450 °C. However, it is noted as two degradation steps and only 85% weight loss was occurred even at 900 °C in the case of silver nanocomposite hydrogel. The weight loss or difference in decomposition between the hydrogel and silver nanocomposite hydrogel is found to be 13% and it illustrates the presence of silver nanoparticles (weight loss) in the hydrogel.

3.5. Particle size analysis

Silver nanoparticles are extracted from hydrogel by swelling the hydrogel for 24 h and the particles are analyzed for particle size analysis. Fig. 5, describes the narrow distribution of particles with average particle size of 15 nm.

3.6. Scanning electron microscopy studies

To confirm the formation of silver nanoparticles and its morphology in hydrogels, the samples were analyzed with a scanning electron microscope. Fig. 6 demonstrates the SEM images of semi-IPN hydrogel–silver nanocomposites. The hydrogel showed branches and rough surface (Fig. 6a), whereas a group of silver nanoparticles were seen in the branches of the hydrogel. The silver nanoparticles are having uniform distribution and size is around 10–20 nm. However, there is a pinpoint variation in the case of silver nanoparticles formed in the gel networks which illustrate the formation of defined nanostructures in the hydrogel networks (Fig. 6b and c). This clearly indicates that formation of silver nanoparticles along with the polymer chains rather than just entrapment in the gel networks. It is quite common that the control or alignment of nanoparticles can be achieved by modifying the hydrogel network architectures.

3.7. Transmisson electron microscopy studies

TEM image demonstrates a highly uniform distribution of silver nanoparticles as shown in Fig. 7. It is confirmed that the silver nanoparticles formed in the crosslinked networks are spherical, highly dispersed, low nanometer in size. Moreover, the electron diffraction (SAED) pattern of silver nanoparticles is clearly visible

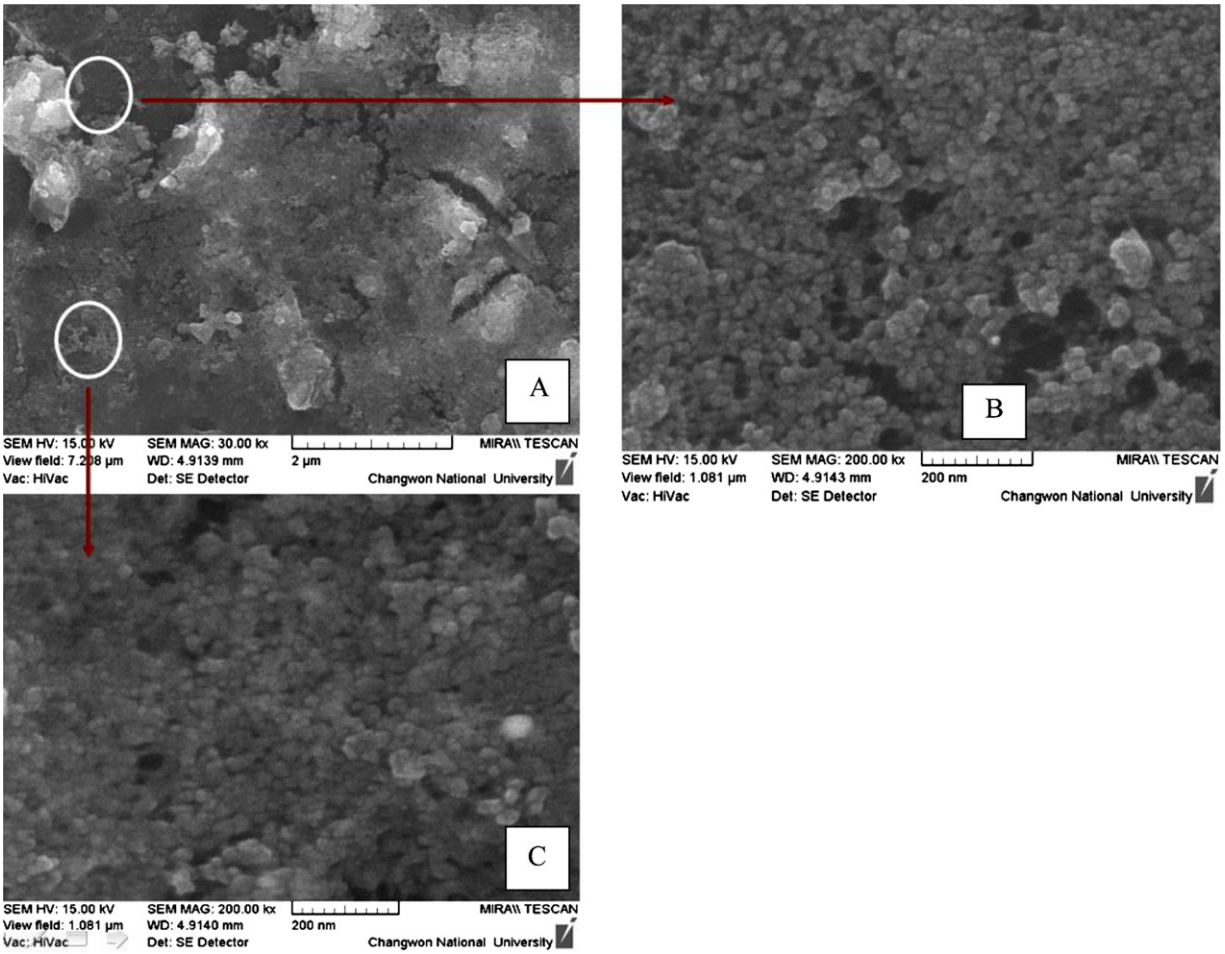

Fig. 6. Scanning electron microscopy images of silver nanocmposite (A) and silver nanoparticles in silver nanocomposite hydrogels (B and C).

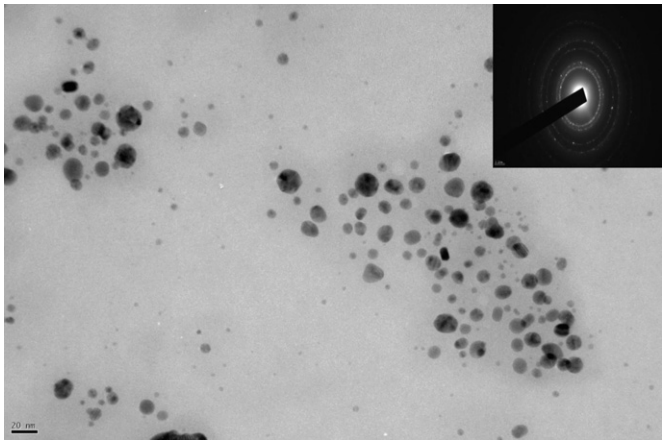

Fig. 7. Typical transmission electron microscopy image of silver nanoparticles.

as three diffraction rings from the selected area of the TEM image and they are definitely attributed to the face-centered cubic structure of silver nanoparticles. The brightest ring and the one closest to the center is a combination of the {1 1 1} and {2 0 0} reflections. The second ring belongs to {2 2 2} reflection and the weakest third ring is due to either {4 2 0} and/or {4 2 2} reflections. This clearly represents that highly dense semi-IPN hydrogel networks favor silver nanoparticle formation because that composition [what is that composition] permits the establishment of inter- and intramolecular attractions between the semi-IPN hydrogel networks due to less free space in the hydrogel networks. The particle size is found between 10 and 20 nm.

3.8. Antibacterial studies

Fig. 8 reveals with the *in vitro* antibacterial screening of semi-IPN hydrogel and its silver analogue which have been carried out against *E. coli*. The results suggest that the silver nanocomposite hydrogel showed more toxic effect on *E. coli* than placebo hydrogel under similar conditions. The possible mode of increased toxicity of silver–hydrogel may be due to the silver nanoparticles could come out easily and could interact with lipid layer of cell membrane.

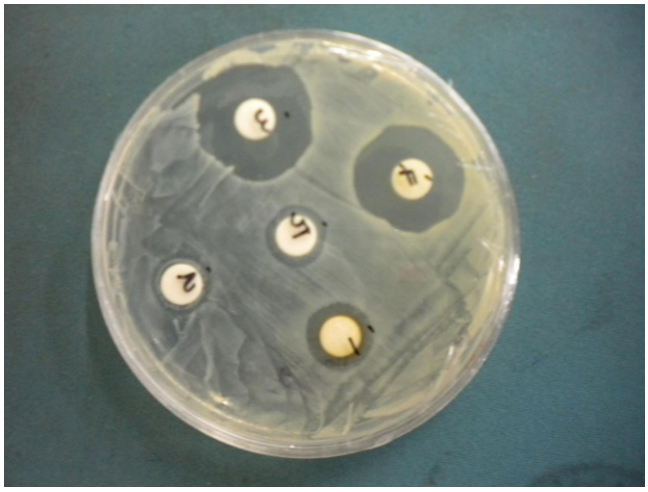

Fig. 8. Antibacterial effect of sample 1 (NAHEMA-1), sample 2 (NAHEMA-2), sample 3 (NAHEMA-3), sample 4 (NAHEMA-4) and sample 5 (NAHEMA-5) silver nanocomposite hydrogels.

4. Conclusions

To summarize, we succeeded in the synthesis of silver nanoparticles in semi-IPN carbohydrate polymeric hydrogel using reduction technique. This technique could be extended to the growth of other type of nanoparticles such as gold nanoparticles. Swelling properties of the hydrogels were different with varying the ratio of polymer and crosslinking agent. Small and uniform silver nanoparticles have been successfully produced through the reduction of silver ions in nanocomposite hydrogel environment. UV analysis exhibits a peak at 400 nm and thermal analysis gave 9% of weight losss difference between hydrogel and silver nanocomposite hydrogel, which reveals the formation of silver nanoparticles in the hydrogel matrix. Scanning electron microscopy and transmission electron microscopy images showed the narrow distribution and spherical shape of silver nanoparticles with size range of 10–20 nm. The developed nanoparticles are showed antibacterial activity and it can be used as drug.

Acknowledgement

The authors gratefully acknowledge the support by the Korea Research Foundation (Grant No. KRF-2007-J00903).

References

Acharya, H., Sung, J., Shin, H., Park, S. Y., Min, B. G., & Park, C. (2009). Deposition of silver nanoparticles on single wall carbon nanotubes via a self assembled block copolymer micelles. *Reactive & Functional Polymers*, *69*, 552–557.
Aminabhavi, T. M., Kulkarni, A. R., Soppimath, K. S., Dave, A. M., & Mehta, M. H. (1999). Applications of sodium alginate beads crosslinked with glutaraldehyde for controlled release of pesticides. *Polymer News*, *24*, 285–286.
Anstas, P. T., & Warner, J. C. (1998). *Green Chemistry: Theory and Practice*. New York: Oxford University Press, Inc.
Binder, W. H., & Heinrich, G. (2000). Block copolymers derived from photoreactive 2-oxazolines, 1. Synthesis and micellization behavior. *Macromolecular Chemistry and Physics*, *201*, 949–957.
Cai, Z., Shi, Z., Sherman, M., & Sun, A. M. (1989). Development and of evaluation of a system of microencapsulation of primary rat hepatocytes. *Hepathology*, *10*, 855–860.
Chegel, V. I., Raitman, O. A., Lioubashevski, O., Shirshov, Y., Katz, E., & Willner, I. (2002). Redox-switching of electrorefractive, electrochromic, and conductivity functions of Cu^{2+}/polyacrylic acid films associated with electrodes. *Advanced Materials*, *14*, 1549–1553.
Chen, W., Cai, W., Zhang, L., Wang, G., & Zhang, L. (2001). Sonochemical Processes and Formation of Gold Nanoparticles within Pores of Mesoporous Silica. *Journal of Colloidal and Interface Science*, *238*, 291–295.
Chou, K. S., & Ren, C. Y. (2000). Synthesis of nanosized silver particles by chemical reduction method. *Material Chemistry Physics*, *64*, 241–246.
Cross, R. A., & Kalra, B. (2002). Biodegradable Polymers for the Environment. *Science*, *297*, 803–807.
Dahl, J. A., Bettye, L., Maddux, S., & Hutchison, J. E. (2007). Toward Greener Nanosynthesis. *Chemical Reviews*, *107*, 2228–2269.
DeSimone, J. M. (2002). Practical Approaches to Green Solvents. *Science*, *297*, 799–803.
Downs, E. C., Robertson, N. E., Riss, T. L., & Plunkett, M. I. J. (1992). Calcium alginate beads as a slow-release system for delivering angiogenic molecules in vivo and *in vitro*. *Journal of Cellular Physiology*, *152*, 422–429.
Frattini, A., Pellegri, N., Nicastro, D., & DeSanctis, O. (2005). *Material Chemistry Physics*, *94*, 148–156.
Henglein, A. (1989). Small-particle research: Physicochemical properties of extremely small colloidal metal and semiconductor particles. *Chemical Reviews*, *89*, 1861–1873.
Hertzberg, S., Moen, E., Vogelsang, C., & Oestgaard, K. (1995). Mixed photo-crosslinked polyvinyl alcohol and calcium-alginate gels for cell entrapment. *Applied Microbiology and Biotechnology*, *43*, 10–17.
Hutchison, J. E. (2008). Greener nanoscience: A proactive approach to advancing applications and reducing implications of nanotechnology. *ACS Nano*, *2*, 395–402.
Kang, D. W., Choi, H. R., & Kweon, D. K. (1999). Stability constants of amidoximated chitosan-g-poly(acrylonitrile) copolymer for heavy metal ions. *Journal of Applied Polymer Science*, *73*, 469–476.
Kapoor, S., Lawless, D., Kennepohl, P., Meisel, D., & Serpone, N. (1994). Reduction and Aggregation of Silver Ions in Aqueous Gelatin Solutions. *Langmuir*, *10*, 3018–3022.
Knoll, B., & Keilmann, F. (1999). Near-field probing of vibrational absorption for chemical microscopy. *Nature*, *399*, 134–137.

Lee, W. F., & Chen, Y. J. (2001). Studies on preparation and swelling properties of the *N*-isopropylacrylamide/chitosan semi-IPN and IPN hydrogels. *Journal of Applied Polymer Science*, *82*, 2487–2496.

Lim, F., & Moss, R. D. (1981). Microencapsulation of living cells and tissues. *Journal of Pharmaceutical Sciences*, *70*, 351–354.

Ng, L. T., Yuan, Y. J., & Zhao, H. (1998). Natural Polymer-Based Sulfite Biosensor. *Electroanalysis*, *10*, 1119–1124.

Nickel, U., Castell, Z., Poppl, K., & Schneider, S. (2000). A Silver Colloid Produced by Reduction with Hydrazine as Support for Highly Sensitive Surface-Enhanced Raman Spectroscopy. *Langmuir*, *16*, 9087–9091.

Park, S. B., You, J. O., Park, H. Y., Haam, S. J., & Kim, W. S. (2001). A novel pH-sensitive membrane from chitosan-TEOS IPN; preparation and its drug permeation characteristics. *Biomaterials*, *22*, 323–330.

Peniche, C., Monal, W. A., Davidenko, N., Sastre, R., Gallardo, A., & Roman, J. S. (1999). Self-curing membranes of chitosan/PAA IPNs obtained by radical polymerization: Preparation, characterization and interpolymer complexation. *Biomaterials*, *20*, 1869–1878.

Poliakoff, M., & Anastas, P. (2001). A Principled Stance. *Nature*, *413*, 257–1257.

Ramesh Babu, V., Krishna Rao, K. S. V., Sairam, M., Naidu, B. V. K., Hosamani, K. M., & Aminabahvi, T. M. (2006). pH-Sensitive interpenetrating network microgels of sodium alginateacrylic acid for the controlled release of ibuprofen. *Journal Applied Polymer Science*, *99*, 2671–2678.

Ramesh Babu, V., Sairam, M., Hosamani, K. M., & Aminabahvi, T. M. (2007). Preparation of sodium alginate-methyl cellulose blend microspheres for controlled release of nifedipine. *Carbohydrate Polymers*, *69*, 241–250.

Ramesh Babu, V., Hosamani, K. M., & Aminabahvi, T. M. (2008). Preparation and in vitro release of chlorothiazide novel pH-sensitive chitosan-*N*′,*N*′-dimethylacrylamide semi-interpenetrating network microspheres. *Carbohydrate Polymers*, *71*, 208–217.

Raveendran, P., Fu, J., & Wallen, S. L. (2003). Completely "Green" Synthesis and Stabilization of Metal Nanoparticles. *Journal of American Chemical Society*, *125*, 13940–13941.

Sastre, R. L., Blanco, M. D., Gomez, C., Socorro, J. M. D., & Teijon, J. M. (1999). Cytarabine trapping in poly(2-hydroxyethyl methacrylate-*co*-acrylamide) hydrogels: Drug delivery studies. *Polymer International*, *48*, 843–850.

Shiladitya, S., Eavarone, D., Capila, I., Zhao, G., Watson, N., Kiziltepe, T., & Sasisekharan, R. (2005). Temporal targeting of tumour cells and neovasculature with a nanoscale delivery system. *Nature*, *436*, 568–572.

Shirtcliffe, N., Nickel, U., & Schneider, S. (1999). Reproducible Preparation of Silver Sols with Small Particle Size Using Borohydride Reduction: For Use as Nuclei for Preparation of Larger Particles. *Journal of Colloid Interface Science*, *211*, 122–129.

Tao, A., Sinsermsuksakul, P., & Yang, P. (2006). Polyhedral Silver Nanocrystals with Distinct Scattering Signatures. *Angewandte Chemie International Edition*, *45*, 4597–4601.

Whitcombe, M. J., & Vulfson, E. N. (2001). Imprinted Polymers. *Advanced Materials*, *13*, 467–478.

Wiley, B., Sun, Y., & Xia, Y. (2007). Synthesis of Silver Nanostructures with Controlled Shapes and Properties. *Accounts of Chemical Research*, *40*, 1067–1076.

Wiley, B., Sun, Y., Mayers, B., & Xia, Y. (2005). Shape-Controlled Synthesis of Metal Nanostructures: The Case of Silver. *Chemistry—A European Journal*, *11*, 454–463.